



Published in final edited form as:

ACS Chem Biol. 2016 April 15; 11(4): 1012–1018. doi:10.1021/acscchembio.5b00899.

## Synthetic ROR $\gamma$ t Agonists Enhance Protective Immunity

Mi Ra Chang, Venkatasubramanian Dharmarajan, Christelle Doebelin, Ruben D. Garcia-Ordonez, Scott J. Novick, Dana S. Kuruvilla, Theodore M. Kamenecka, and Patrick R. Griffin  
Department of Molecular Therapeutics, The Scripps Research Institute, Scripps Florida, Jupiter, FL33458, USA

### Abstract

The T cell specific ROR $\gamma$  isoform ROR $\gamma$ t has been shown to be the key lineage-defining transcription factor to initiate the differentiation program of T<sub>H</sub>17 and T<sub>C</sub>17 cells, cells that have demonstrated anti-tumor efficacy. ROR $\gamma$ t controls gene networks that enhance immunity including increased IL17 production and decreased immune suppression. Both synthetic and putative endogenous agonists of ROR $\gamma$ t have been shown to increase the basal activity of ROR $\gamma$ t enhancing T<sub>H</sub>17 cell proliferation. Here we show that activation of ROR $\gamma$ t using synthetic agonists drives proliferation of T<sub>H</sub>17 cells while decreasing levels of the immune checkpoint protein PD-1, a mechanism that should enhance anti-tumor immunity while blunting tumor associated adaptive immune resistance. Interestingly, putative endogenous agonists drive proliferation of T<sub>H</sub>17 cells but do not repress PD-1. These findings suggest that synthetic agonists of ROR $\gamma$ t should activate T<sub>C</sub>17/T<sub>H</sub>17 cells (with concomitant reduction in the Tregs population), repress PD-1, and produce IL17 *in situ* (a factor associated with good prognosis in cancer). Enhanced immunity and blockage of immune checkpoints has transformed cancer treatment, thus such a molecule would provide a unique approach for the treatment of cancer.

### Keywords

nuclear receptor; agonist; retinoic acid receptor-related orphan receptor gamma; ROR $\gamma$ t; hydrogen/deuterium exchange; HDX; protective immunity; immunotherapy

Corresponding Author: Patrick R. Griffin, PhD, The Scripps Research Institute, Scripps Florida, 130 Scripps Way #2A2, Jupiter, FL33458, pgriffin@scripps.edu.

Supporting Information: This manuscript contains three supplemental figures and two supplemental tables. The material contained in the supporting information is listed below.

- Chemical structures of SR1078, SR0987, SR2211, ursolic acid, and desmosterol.
- CRC for SR1078 and SR2211 in the presence of ursolic acid (2 $\mu$ M) in the Gal4-ROR $\gamma$ ::UAS-Luc reporter assay in HEK293T cells.
- CRC for SR1078, SR0987, and SR2211 in a TR-FRET assay using ROR $\gamma$  LBD and a FITC labeled SRC1 NR BOX 1 peptide.
- Differential HDX perturbation Tables; a) Differential HDX Kinetics of ROR $\gamma$ t  $\pm$  Compounds. b) Differential HDX Kinetics of ROR $\gamma$ t pretreated with ursolic Acid  $\pm$  Compounds.
- Primer sequence for Q-PCR analysis.

The nuclear receptor (NR) superfamily of transcription factors has proven to be rich source of targets for development of therapeutics for a myriad of human diseases. In addition to control by cellular localization and PTM status, the transcriptional activity of most NRs can be modulated (activated or repressed) by small lipophilic molecules such as hormones, vitamins, steroids, oxysterols, retinoids, fatty acids, and synthetic molecules<sup>1</sup>. The NR1F subfamily of NRs contains the retinoic acid receptor-related orphan receptors (RORs) that include ROR $\alpha$ , ROR $\beta$ , and ROR $\gamma$ . These receptors have been shown to regulate a wide range of physiological processes, have been implicated in the pathophysiology of disease, and their basal activity can be modulated by sterols<sup>2-4</sup>.

The T cell specific isoform of ROR $\gamma$ , known as ROR $\gamma$ t, is expressed in thymocytes and regulates survival of T cells during differentiation<sup>5</sup> and drives the activation and differentiation of CD4<sup>+</sup> and CD8<sup>+</sup> cells into IL17-producing helper T cells (T<sub>H</sub>17) and cytotoxic T cells (Tc17)<sup>6</sup>. T<sub>H</sub>17 and Tc17 are effector cells that promote inflammation, adaptive immunity and autoimmunity by producing IL17 and other inflammatory cytokines such as IL21. Since T<sub>H</sub>17 cells do not express granzyme B or perforin and do not appear to have a direct effect on cancer cell proliferation and apoptosis, it is thought that these cells may not mediate direct cytotoxic activity against tumors<sup>7, 8</sup>.

The programmed cell death 1 receptor PD-1 can inhibit T cell activation when bound by the ligand PD-L1. Tumor expression of PD-L1 leads to an inactivation of a T cell immune response to the cancer cells. Activated T cells produce interferon and stimulate PD-L1 on tumor cells and the PD-1/PD-L1 interaction triggers a process that shuts down the immune response reducing proliferation of these effector cells. In the tumor microenvironment, T cells overexpress PD-1 and act in concert to blunt T cell antitumor effects<sup>9, 10</sup>. Among the most promising approaches to activating therapeutic antitumor immunity is the blockade of immune checkpoints. While T<sub>H</sub>17 cells have a well described role in autoimmune disease, recent evidence suggests that this subset of effector T cells may play a role in immunotherapy if the PD-1 pathway is inactivated<sup>11</sup>. Enhanced immunity through T-cell activation and blockage of immune checkpoints has transformed cancer treatment with therapies targeting PD-1 showing unprecedented rates of durable clinical responses in patients with various cancers<sup>12-16</sup>.

Several reports have described ROR $\gamma$ t synthetic agonists including SR1078, a compound that induced the expression of the ROR target genes *FGF21* and *G6Pase* in cells and *in vivo*<sup>17-19</sup>. In Rene *et al*, the authors show that a minor substitution of a phenylsulfonamide for a benzylsulfonamide within the same chemical scaffold changes the compound from an inverse agonist to an agonist on ROR $\gamma$ t with no activity on ROR $\alpha$ <sup>19</sup>. Co-crystal structures of the benzylsulfonamide and phenylsulfonamide derivatives bound to ROR $\gamma$ t provided further structural insights into the opposing MOA of these compounds. These studies clearly demonstrate that it is possible to upregulate basal ROR $\gamma$ t activity with synthetic modulators.

Our recent efforts to optimize the SR1078 scaffold provided many analogs with improved biochemical and physiochemical properties. These compounds were evaluated for their ability to positively modulate IL17 to aid activation of T<sub>H</sub>17 cells and for their ability to impact PD-1 cell surface expression. Here we show that activation of ROR $\gamma$ t with the

SR1078 analog SR0987, leads to increased expression of IL17 while repressing the expression of the checkpoint receptor PD-1, activities that the recently identified endogenous sterol agonists do not engender.

## Results and Discussion

Competitive radioligand binding assays illustrated direct binding of SR1078 to the ligand binding domain (LBD) of ROR $\gamma$ t albeit with weak affinity ( $IC_{50} \sim 15 \mu\text{M}$ )<sup>18</sup>. SR1078 was also shown to have direct interaction with ROR $\gamma$ t via thermal shift assay as measured by Circular Dichroism (CD)<sup>17</sup>. The lack of potency in displacing the radiolabeled orthosteric inverse agonist T0901317 is likely due to SR1078 binding in the recently described allosteric pocket on ROR $\gamma$ t<sup>20</sup>. Initial SAR of the benzamide ring suggests that substituents are tolerated at the ortho-position leading to SR0987 (Fig. 1a and Supplementary Fig. 1). Compounds were subsequently screened in a Gal4 UAS-Luc cotransfection system in order to determine their ability to modulate ROR $\gamma$  activity in a cellular environment. Given that ROR $\gamma$ t has high basal activity when expressed in cells, repression by the receptors' activity using an inverse agonist (e.g., ursolic acid) followed by test compound treatment offered the best window to detect agonism<sup>3</sup>. Here cells were pre-treated with 2  $\mu\text{M}$  ursolic acid ( $IC_{50} \sim 0.8 \mu\text{M}$ ) which afforded approximately 60–70% of ROR $\gamma$ t activity prior to the addition of test compounds. Desmosterol was used as a control for agonism as it was recently identified as a putative endogenous agonist for ROR $\gamma$ t capable of restoring ROR $\gamma$ t activity in the presence of ursolic acid. Importantly, in this assay format, the potent inverse agonist SR2211<sup>21, 22</sup> demonstrated the ability to further repress the expression of the luciferase reporter gene in the presence of ursolic acid (Supplementary Fig. 2). Initial screening of compounds was performed at a single concentration of 30  $\mu\text{M}$  looking for compounds with improved reporter gene expression relative to desmosterol. In this screening format SR0987 afforded the highest fold induction of reporter gene expression (~6 fold), whereas desmosterol and SR1078 resulted in only a minor induction of luciferase expression (~2 fold) (Fig. 1b). Furthermore, SR0987 clearly shows a concentration dependent induction of reporter gene expression with an  $EC_{50}$  of ~800nM (Fig. 1c). Interestingly, desmosterol only induced luciferase expression at the highest concentration tested (~2 fold at 30  $\mu\text{M}$ ). The concentration response curve for SR1078 is shown in Supplementary Fig. 2 confirming the improved agonist activity of SR0987. In addition, as shown in Supplementary Fig. 3, SR1078 and SR0987 demonstrate concentration dependent increase in interaction of ROR $\gamma$ t with the SRC1-3 NR box peptide further validating that these compounds drive the agonist conformation of the receptor. As expected, SR2211 decreases interaction with this co-activator peptide in a concentration dependent fashion.

In order to determine if these compounds could modulate ROR $\gamma$ t activity in the context of the full-length receptor, we used a co-transfection system in HEK293T cells in which full length ROR $\gamma$ t was co-transfected along with a luciferase reporter under the control of either a basic promoter containing five copies of an ROR response element (5xRORE) or a minimal IL17 promoter. For all subsequent *in vitro* pharmacology studies we focused on the more efficacious synthetic agonist SR0987. As shown in Fig. 1d and 1e, SR0987 demonstrated a concentration-dependent induction of reporter gene expression in both the 5xRORE and IL17 promoter transfected cells in the presence of full-length ROR $\gamma$ t whereas

minimal induction of the reporter gene was observed with desmosterol treatment. As expected, the inverse agonist SR2211 repressed both promoters in a concentration-dependent manner.

PD-1 is not expressed on resting T cells but its expression is induced within 24 hours after T cell receptor stimulation<sup>23</sup> and is involved in the establishment and maintenance of immunological tolerance in the spontaneous development of autoimmune diseases by PD-1 deficient mice<sup>24, 25</sup>. Given that PD-L1 is expressed on various tumor cells and PD-1 expression is upregulated and sustained on T cells, it is clear that the PD-1/PD-L1 pathway plays an important role in tumor immunity. Here we used murine EL4 T lymphocytes or human Jurkat T cells as model systems to analyze gene expression upon T cell activation. Following treatment of cells with Phorbol 12-myristate 13-acetate (PMA) and ionomycin, the expression of *granzyme B* (cytotoxicity marker), *PD-1* (immune checkpoint) and the ROR $\gamma$ t target gene *IL17* were analyzed by qPCR. As shown in Fig. 2a stimulation of EL4 cells led to an increase in the expression of all three genes and when coupled with treatment with the synthetic ROR $\gamma$ t agonist SR0987 a further increase in expression of *IL17* was observed suggesting that there was induction of T cell activation. Surprisingly and unexpectedly, treatment with SR0987 led to a decrease in expression of PD-1. Compound treatment did not impact the expression of *granzyme B*. Combined these results suggest that treatment with SR0987 may enhance protective immunity by regulating expression of *IL17* and PD-1 while maintaining the cytotoxic ability of these cells.

Using flow cytometry, surface PD-1 expression was analyzed to determine if the decrease in gene expression of PD-1 correlate to a decrease of the protein on the cell surface. Cell surface PD-1 expression was measured in murine and human T cell lines as well as in *ex vivo* differentiated murine T<sub>H</sub>17 cells. SR0987 treatment resulted in a statistically significant reduction of the surface expression of PD-1 whereas desmosterol treatment showed no effect (Fig. 2b). Next we examined the impact of compound treatment on differentiated murine T<sub>H</sub>17 cells. Treatment with SR0987 and or desmosterol resulted in a trend towards increased *IL17* production (Fig. 2c). However, in this system SR0987 again demonstrated the ability to repress surface PD-1 expression whereas desmosterol had no effect (Fig. 2d). To determine if there was an increase in the active T cell population during T<sub>H</sub>17 cell differentiation, the population of CD62L<sup>-</sup>PD1<sup>-</sup> double negative cells was measured using flow cytometry. Naïve CD4<sup>+</sup> T cells isolated from mice were differentiated using a cytokine cocktail in the presence or absence of ursolic acid. SR0987 resulted in a statistically significant increase in the CD62L<sup>-</sup>PD1<sup>-</sup>CD4<sup>+</sup> cell population as compared when compared to DMSO treated cells (Fig. 2e). To determine if the effects of SR0987 on PD-1 expression would be observed in a human cell line, Jurkat T cells were treated with the compound. As shown in Fig. 2f, exposure of Jurkat T cells to SR0987 resulted in decreased cell surface PD-1 expression (Fig. 2f).

Taken together, these results suggest that SR0987 acts as a ROR $\gamma$ t agonist and that use of such synthetic ligands may enhance immune response in the context of cancer. While the mechanism of action of ROR $\gamma$ t agonists on regulation of the immune checkpoint receptor PD-1 is unclear, a correlation between ROR $\gamma$ t and PD-1 expression has been observed in PD-1 knockout mice<sup>26</sup>. Regardless, to gain insights into the structural mechanism for

agonist activity we examined the impact of putative agonist ligands on the conformational dynamics of ROR $\gamma$ t. To achieve this, we utilized differential hydrogen/deuterium exchange (HDX) mass spectrometry. Previously, we have demonstrated the utility of HDX to monitor ligand-induced conformational changes in NRs including ROR $\gamma$ t<sup>27–29</sup>. The differential HDX kinetics of ROR $\gamma$ t LBD in the absence and presence of ursolic acid (inverse agonist), SR2211 (inverse agonist), and desmosterol (putative endogenous agonist) are shown overlaid on the 25- $\alpha$ -OHC:ROR $\gamma$  co-crystal structure (PDB ID: 3L0L)<sup>30</sup> (Fig. 3a). HDX revealed that helix 11 (H11) shows increased protection to solvent exchange (stabilization) with all ROR $\gamma$ t ligands tested, suggesting common sites of direct interaction for ligands within the ligand-binding pocket (LBP) of ROR $\gamma$ t. No statistically significant change in HDX kinetics was observed in the activation function-2 helix, helix 12 (H12), for these three complexes (Supplementary Table 1a). In contrast, Fig. 3b shows differential HDX kinetics of ROR $\gamma$ t exposed to ursolic acid followed by addition of desmosterol (putative endogenous agonist), SR1078 (agonist) and SR0987 (agonist) also overlaid on PDB ID: 3L0L. Protection to solvent exchange was again observed in H11; In addition, treatment with either SR1078 or SR0987, induced protection to solvent exchange in H12 that was not observed with desmosterol (Supplementary Table 1b). This observation is consistent with the concentration-dependent activation of ROR $\gamma$ t observed in cells with these two synthetic agonists and is also consistent with both these synthetic agonists binding in an allosteric pocket as opposed to desmosterol that binds in the orthosteric pocket<sup>20</sup>. Similar agonist induced H12 protections have been previously observed with other NRs such as PPAR $\gamma$ <sup>29</sup>. The differential patterns of H12 protection seen between agonists and inverse agonist are in line with the recently published crystal structures of ROR $\gamma$ t-LBD in complex with synthetic inverse agonist and a synthetic agonist (PDB ID: 4WQP and 4WPF)<sup>19</sup>. These structures revealed that synthetic agonists pack against H3 and H11/12 interface and engages with ROR $\gamma$ t LBD residues Trp317 (H3), His479 (H11) and Tyr502 (H12) resulting in a stable H12 conformation through a direct hydrogen bond between His479 and Tyr502 side chains. Whereas a synthetic inverse agonist dislodges His479 side chain into an orientation that is unfavorable for forming the hydrogen bond with Tyr502, which destabilized H12 (disordered in the structure) and disrupted co-activator interactions. Collectively, the HDX studies provide a structural basis for the agonist properties of SR0987.

Enhanced immunity and blockage of immune checkpoints has transformed cancer treatment with therapies targeting PD-1 showing unprecedented rates of durable clinical responses in patients with various cancers. The results presented here suggest that ROR $\gamma$  agonists may enhance T cell activation while repressing PD-1 without reducing the cytotoxic activity of these cells. Therefore, ROR $\gamma$  agonists may provide a unique combination therapy with approved anti-PD-1 molecules for treatment of cancer and may provide utility in the context of anti-PD-1 resistance.

## Methods

### Compounds

Chemicals and solvents were purchased from commercial suppliers. Compounds were purified using CombiFlash Rf 200 flash chromatography on silica gel on RediSEp Rf from

Teledyne Isco, Inc. Yields refer to isolated compounds, estimated to be > 98% pure as determined by  $^1\text{H}$  NMR or HPLC. Melting points were measured on a Stuart automatic melting point SMP40.  $^1\text{H}$ ,  $^{13}\text{C}$  NMR spectra were recorded on Bruker Spectrometer operating at 400 MHz and 101 MHz respectively. All chemical shift values,  $\delta$ , and coupling constants,  $J$ , are quoted in ppm and Hz, respectively. Infra-Red spectrums were recorded on Perkin Elmer FT-IR Spectrometer.

Synthesis of SR1078 was performed as previously described<sup>18</sup>. Synthesis of SR0987: To a solution of 4-(1-hydroxy-1-trifluoromethyl-2,2,2-trifluoroethyl)aniline (60mg, 0.232 mmol) in  $\text{CH}_2\text{Cl}_2$  (2 mL) were successively added at RT *N,N*-diisopropylethylamine (80  $\mu\text{L}$ , 0.463 mmol) and 2-chlorobenzoyl chloride (41  $\mu\text{L}$ , 0.324 mmol). The mixture was stirred for 3 h and concentrated under reduce pressure. The crude residue was directly purified by column chromatography on silica gel without any workup by hexane/AcOEt (8/2) to obtain 65 mg (71%) of SR0987 as a white powder: FTIR  $\text{cm}^{-1}$  3338, 3028, 1643, 1521, 1410, 1254, 1219, 1188, 1112, 968, 944, 826;  $^1\text{H}$  NMR (400 MHz, MeOD- $d_4$ )  $\delta$  = 7.97 (t,  $J$  = 1.8 Hz, 1 H), 7.91 - 7.86 (m, 1 H), 7.85 - 7.80 (m, 2 H), 7.75 - 7.70 (m, 2 H), 7.63 - 7.58 (m, 1 H), 7.51 (t,  $J$  = 7.8 Hz, 1 H);  $^{13}\text{C}$  NMR (101 MHz, MeOD- $d_4$ )  $\delta$ ; = 167.5, 141.5, 138.2, 135.9, 133.1, 131.4, 129.0 (2C), 128.9, 128.5, 127.3 (2C), 121.7 There are three carbons missing for the description of SR0987. They correspond to the three carbons of the (1-hydroxy-1-trifluoromethyl-2,2,2-trifluoroethyl) moiety. The fluorine coupling with these carbons give multiplets that are very difficult to see on the  $^{13}\text{C}$  spectrum even with a prolonged number of scans. HRMS (ESI)  $m/z$  [ $\text{M}+\text{H}^+$ ] calculated for  $\text{C}_{16}\text{H}_{10}\text{ClF}_6\text{NO}_2$ , 398.0377; found, 398.0395; Mp = 170–172°C. Sterols were purchased from Avanti Polar Lipids and all other chemicals were purchased from Sigma.

## HDX-MS

Solution-phase amide HDX was performed with a fully automated system as described previously with minor modifications<sup>31, 32</sup>. For differential HDX experiments, 5 $\mu\text{L}$  of a 10 $\mu\text{M}$  ROR $\gamma\text{t}$  LBD solution (Apo or in complex with 10-excess compound) was diluted to 25 $\mu\text{L}$  with  $\text{D}_2\text{O}$ -containing HDX buffer, and incubated at 4°C for; 10s, 30s, 60s, 900s, and 3,600s. Following on-exchange, unwanted forward or back exchange is minimized and the protein is denatured by dilution to 50 $\mu\text{L}$  with 0.1% TFA in 3M urea (held at 4° C, pH 2.5). Samples are then passed across an immobilized pepsin column (prepared in house) at 50 $\mu\text{L}$  min $^{-1}$  (0.1% TFA, 15°C) and the resulting peptides are trapped onto a  $\text{C}_8$  trap cartridge (Thermo Fisher, Hypersil Gold). Peptides were then gradient eluted (4%  $\text{CH}_3\text{CN}$  to 40%  $\text{CH}_3\text{CN}$ , 0.3% formic acid over 5 minutes, 4°C) across a 1mm x 50mm  $\text{C}_{18}$  HPLC column (Hypersil Gold, Thermo Fisher) and electrosprayed directly into a high resolution orbitrap mass spectrometer (Exactive, Thermo Fisher). Percent deuterium exchange values for peptide isotopic envelopes at each time point were calculated and processed using HDX Workbench<sup>33</sup> and overlaid onto ROR $\gamma\text{t}$  crystal structures using pyMOL (DeLano Scientific). HDX data is presented as an average of three individual replicates across 6 time points (10s, 60s, 300s, 900s, and 3600s).



### NR box peptide interaction assay

A TR-FRET-based interaction assay was used. The His-Sumo ROR $\gamma$  ligand binding domain (LBD) and FITC-labeled SRC1-3 peptide (sequence: ASNLGLEDIIRKALMGSD $\gamma$ ) was used. TR-FRET reaction contains 2.5nM ROR $\gamma$  LBD, 450nM SRC1-3 peptide in assay buffer (TR-FRET Coregulator Buffer D, Life Technologies). The mixtures were incubated for 2hr at R.T., and fluorescence intensity was measured on an Envision plate reader with excitation at 340nm and emission at 490nm and 520 nm. The ratio of intensity at 520 nm/490nm was used to calculate cofactor recruitment activity.

### Luciferase reporter assay

HEK 293T cells were transfected with a UAS: luciferase reporter and a Gal4-ROR $\gamma$  encoding plasmid (using X-trememGENE 9, Roche). Cells were pre-treated with ursolic acid before compounds were added. Luciferase activity was measured 20 hr after compound addition.

### Gene expression and Cell sorting

Jurkat T cells were pre-incubated with compounds for 48 hr and activated with phorbol 12-myristate 13-acetate (PMA, 50 ng/mL; Sigma) and ionomycin (1 $\mu$ g/mL; Sigma) for 5hr. For qPCR, mRNA was isolated with an RNeasy midi kit using DNase I (Qiagen), and cDNA was synthesized with high capacity cDNA Reverse Transcription kit (Applied Biosystems). IL17A, PD-1, and granzyme B gene expression were normalized to the expression of GAPDH. The sequence of primers used in this study are found in Supplemental Table 2. For cell sorting, activated Jurkat T cells were stained with APC conjugated anti-human PD-1 antibody (eBioscience). Cell sorting was performed using LSRII (BD Bioscience).

### T<sub>H</sub>17 cell differentiation

For naïve T cell differentiation, CD4<sup>+</sup>T cells were enriched by negative selection using a magnetic-activated cell sorter kit (Millipore). Enriched CD4<sup>+</sup> T cells activated with 5 $\mu$ g/mL of plate-bound anti CD3 antibody and 1  $\mu$ g/mL of anti- CD28 antibody in the presence of 20  $\mu$ g/mL of anti- IFN $\gamma$ , 20  $\mu$ g/mL of anti- IL-4, 1ng/mL of TGF $\beta$ , AND 10 ng/mL of IL-6. Four-five days post differentiation, all cells were stimulated for 5 hr with 5 ng/mL of phorbol-12-myristate-13-acetate (Sigma) and 500 ng/mL of ionomycin (Sigma) contained with brefeldin A solution (eBioscience).

### Data analysis and statistics

All experiments were done with three or more biological replicates. Error bars represent standard deviation. Statistics were calculated using an unpaired, two sample Student's t-test.

### Supplementary Material

Refer to Web version on PubMed Central for supplementary material.

## Acknowledgments

We thank B. Pascal for creation of the Graphical Abstract. All authors received funding from the National Institutes of Health, National Institute of Mental Health Grant MH108173.

## Abbreviations

<b>ROR<math>\gamma</math>t</b>	T cell specific retinoic acid receptor-related orphan receptor gamma isoform
<b>HDX</b>	hydrogen/deuterium exchange
<b>LBD</b>	ligand-binding domain

## References

1. Huang Z, Xie H, Wang R, Sun Z. Retinoid-related orphan receptor gamma t is a potential therapeutic target for controlling inflammatory autoimmunity. *Expert opinion on therapeutic targets*. 2007; 11:737–743. [PubMed: 17504012]
2. Wang Y, Kumar N, Solt LA, Richardson TI, Helvering LM, Crumbley C, Garcia-Ordonez RD, Stayrook KR, Zhang X, Novick S, Chalmers MJ, Griffin PR, Burris TP. Modulation of retinoic acid receptor-related orphan receptor alpha and gamma activity by 7-oxygenated sterol ligands. *The Journal of biological chemistry*. 2010; 285:5013–5025. [PubMed: 19965867]
3. Hu X, Wang Y, Hao LY, Liu X, Lesch CA, Sanchez BM, Wendling JM, Morgan RW, Aicher TD, Carter LL, Toogood PL, Glick GD. Sterol metabolism controls T(H)17 differentiation by generating endogenous RORgamma agonists. *Nature chemical biology*. 2015; 11:141–147. [PubMed: 25558972]
4. Santori FR, Huang P, van de Pavert SA, Douglass EF Jr, Leaver DJ, Haubrich BA, Keber R, Lorbek G, Konijn T, Rosales BN, Rozman D, Horvat S, Rahier A, Mebius RE, Rastinejad F, Nes WD, Littman DR. Identification of natural RORgamma ligands that regulate the development of lymphoid cells. *Cell metabolism*. 2015; 21:286–297. [PubMed: 25651181]
5. Sun Z, Unutmaz D, Zou YR, Sunshine MJ, Pierani A, Brenner-Morton S, Mebius RE, Littman DR. Requirement for RORgamma in thymocyte survival and lymphoid organ development. *Science*. 2000; 288:2369–2373. [PubMed: 10875923]
6. Skepner J, Ramesh R, Trocha M, Schmidt D, Baloglu E, Lobera M, Carlson T, Hill J, Orband-Miller LA, Barnes A, Boudjelal M, Sundrud M, Ghosh S, Yang J. Pharmacologic inhibition of RORgamma regulates Th17 signature gene expression and suppresses cutaneous inflammation in vivo. *J Immunol*. 2014; 192:2564–2575. [PubMed: 24516202]
7. Kryczek I, Banerjee M, Cheng P, Vatan L, Szeliga W, Wei S, Huang E, Finlayson E, Simeone D, Welling TH, Chang A, Coukos G, Liu R, Zou W. Phenotype, distribution, generation, and functional and clinical relevance of Th17 cells in the human tumor environments. *Blood*. 2009; 114:1141–1149. [PubMed: 19470694]
8. Yen HR, Harris TJ, Wada S, Grosso JF, Getnet D, Goldberg MV, Liang KL, Bruno TC, Pyle KJ, Chan SL, Anders RA, Trimble CL, Adler AJ, Lin TY, Pardoll DM, Huang CT, Drake CG. Tc17 CD8 T cells: functional plasticity and subset diversity. *J Immunol*. 2009; 183:7161–7168. [PubMed: 19917680]
9. Twyman-Saint Victor C, Rech AJ, Maity A, Rengan R, Pauken KE, Stelekati E, Benci JL, Xu B, Dada H, Odorizzi PM, Herati RS, Mansfield KD, Patsch D, Amaravadi RK, Schuchter LM, Ishwaran H, Mick R, Pryma DA, Xu X, Feldman MD, Gangadhar TC, Hahn SM, Wherry EJ, Vonderheide RH, Minn AJ. Radiation and dual checkpoint blockade activate non-redundant immune mechanisms in cancer. *Nature*. 2015; 520:373–377. [PubMed: 25754329]
10. Gubin MM, Zhang X, Schuster H, Caron E, Ward JP, Noguchi T, Ivanova Y, Hundal J, Arthur CD, Krebber WJ, Mulder GE, Toebes M, Vesely MD, Lam SS, Korman AJ, Allison JP, Freeman GJ, Sharpe AH, Pearce EL, Schumacher TN, Abersold R, Rammensee HG, Melief CJ, Mardis ER, Gillanders WE, Artyomov MN, Schreiber RD. Checkpoint blockade cancer immunotherapy targets tumour-specific mutant antigens. *Nature*. 2014; 515:577–581. [PubMed: 25428507]



11. Zou W, Restifo NP. T(H)17 cells in tumour immunity and immunotherapy. *Nature reviews Immunology*. 2010; 10:248–256.
12. Topalian SL, Hodi FS, Brahmer JR, Gettinger SN, Smith DC, McDermott DF, Powderly JD, Carvajal RD, Sosman JA, Atkins MB, Leming PD, Spigel DR, Antonia SJ, Horn L, Drake CG, Pardoll DM, Chen L, Sharfman WH, Anders RA, Taube JM, McMiller TL, Xu H, Korman AJ, Jure-Kunkel M, Agrawal S, McDonald D, Kollia GD, Gupta A, Wigginton JM, Sznol M. Safety, activity, and immune correlates of anti-PD-1 antibody in cancer. *The New England journal of medicine*. 2012; 366:2443–2454. [PubMed: 22658127]
13. Brahmer JR, Tykodi SS, Chow LQ, Hwu WJ, Topalian SL, Hwu P, Drake CG, Camacho LH, Kauh J, Odunsi K, Pitot HC, Hamid O, Bhatia S, Martins R, Eaton K, Chen S, Salay TM, Alaparthy S, Grosso JF, Korman AJ, Parker SM, Agrawal S, Goldberg SM, Pardoll DM, Gupta A, Wigginton JM. Safety and activity of anti-PD-L1 antibody in patients with advanced cancer. *The New England journal of medicine*. 2012; 366:2455–2465. [PubMed: 22658128]
14. Hamid O, Robert C, Daud A, Hodi FS, Hwu WJ, Kefford R, Wolchok JD, Hersey P, Joseph RW, Weber JS, Dronca R, Gangadhar TC, Patnaik A, Zarour H, Joshua AM, Gergich K, Ellassaiss-Schaap J, Algazi A, Mateus C, Boasberg P, Tumei PC, Chmielowski B, Ebbinghaus SW, Li XN, Kang SP, Ribas A. Safety and tumor responses with lambrolizumab (anti-PD-1) in melanoma. *The New England journal of medicine*. 2013; 369:134–144. [PubMed: 23724846]
15. Wolchok JD, Kluger H, Callahan MK, Postow MA, Rizvi NA, Lesokhin AM, Segal NH, Ariyan CE, Gordon RA, Reed K, Burke MM, Caldwell A, Kronenberg SA, Agunwamba BU, Zhang X, Lowy I, Inzunza HD, Feely W, Horak CE, Hong Q, Korman AJ, Wigginton JM, Gupta A, Sznol M. Nivolumab plus ipilimumab in advanced melanoma. *The New England journal of medicine*. 2013; 369:122–133. [PubMed: 23724867]
16. Topalian SL, Sznol M, McDermott DF, Kluger HM, Carvajal RD, Sharfman WH, Brahmer JR, Lawrence DP, Atkins MB, Powderly JD, Leming PD, Lipson EJ, Puzanov I, Smith DC, Taube JM, Wigginton JM, Kollia GD, Gupta A, Pardoll DM, Sosman JA, Hodi FS. Survival, durable tumor remission, and long-term safety in patients with advanced melanoma receiving nivolumab. *Journal of clinical oncology: official journal of the American Society of Clinical Oncology*. 2014; 32:1020–1030. [PubMed: 24590637]
17. Zhang W, Zhang J, Fang L, Zhou L, Wang S, Xiang Z, Li Y, Wisely B, Zhang G, An G, Wang Y, Leung S, Zhong Z. Increasing human Th17 differentiation through activation of orphan nuclear receptor retinoid acid-related orphan receptor gamma (RORgamma) by a class of aryl amide compounds. *Molecular pharmacology*. 2012; 82:583–590. [PubMed: 22700697]
18. Wang Y, Kumar N, Nuhant P, Cameron MD, Istrate MA, Roush WR, Griffin PR, Burris TP. Identification of SR1078, a synthetic agonist for the orphan nuclear receptors RORalpha and RORgamma. *ACS chemical biology*. 2010; 5:1029–1034. [PubMed: 20735016]
19. Rene O, Fauber BP, de Boenig GL, Burton B, Eidenschek C, Everett C, Gobbi A, Hymowitz SG, Johnson AR, Kiefer JR, Liimatta M, Lockey P, Norman M, Ouyang W, Wallweber HA, Wong H. Minor Structural Change to Tertiary Sulfonamide RORc Ligands Led to Opposite Mechanisms of Action. *ACS medicinal chemistry letters*. 2015; 6:276–281. [PubMed: 25815138]
20. Scheepstra M, Leysen S, van Almen GC, Miller JR, Piesvaux J, Kutilek V, van Eenennaam H, Zhang H, Barr K, Nagpal S, Soisson SM, Kornienko M, Wiley K, Elsen N, Sharma S, Correll CC, Trotter BW, van der Stelt M, Oubrie A, Ottmann C, Parthasarathy G, Brunsveld L. Identification of an allosteric binding site for RORgamma inhibition. *Nature communications*. 2015; 6:8833.
21. Kumar N, Lyda B, Chang MR, Lauer JL, Solt LA, Burris TP, Kamenecka TM, Griffin PR. Identification of SR2211: a potent synthetic RORgamma-selective modulator. *ACS chemical biology*. 2012; 7:672–677. [PubMed: 22292739]
22. Chang MR, Lyda B, Kamenecka TM, Griffin PR. Pharmacologic repression of retinoic acid receptor-related orphan nuclear receptor gamma is therapeutic in the collagen-induced arthritis experimental model. *Arthritis Rheumatol*. 2014; 66:579–588. [PubMed: 24574218]
23. Chemnitz JM, Parry RV, Nichols KE, June CH, Riley JL. SHP-1 and SHP-2 associate with immunoreceptor tyrosine-based switch motif of programmed death 1 upon primary human T cell stimulation, but only receptor ligation prevents T cell activation. *J Immunol*. 2004; 173:945–954. [PubMed: 15240681]

24. Nishimura H, Honjo T, Minato N. Facilitation of beta selection and modification of positive selection in the thymus of PD-1-deficient mice. *The Journal of experimental medicine*. 2000; 191:891–898. [PubMed: 10704469]
25. Nishimura H, Okazaki T, Tanaka Y, Nakatani K, Hara M, Matsumori A, Sasayama S, Mizoguchi A, Hiai H, Minato N, Honjo T. Autoimmune dilated cardiomyopathy in PD-1 receptor-deficient mice. *Science*. 2001; 291:319–322. [PubMed: 11209085]
26. Tarrío ML, Gräbe N, Bu DX, Sharpe AH, Lichtman AH. PD-1 protects against inflammation and myocyte damage in T cell-mediated myocarditis. *J Immunol*. 2012; 188:4876–4884. [PubMed: 22491251]
27. Zhang J, Chalmers MJ, Stayrook KR, Burris LL, Garcia-Ordóñez RD, Pascal BD, Burris TP, Dodge JA, Griffin PR. Hydrogen/deuterium exchange reveals distinct agonist/partial agonist receptor dynamics within vitamin D receptor/retinoid X receptor heterodimer. *Structure*. 2010; 18:1332–1341. [PubMed: 20947021]
28. Solt LA, Kumar N, Nuhant P, Wang Y, Lauer JL, Liu J, Istrate MA, Kamenecka TM, Roush WR, Vidovic D, Schurer SC, Xu J, Wagoner G, Drew PD, Griffin PR, Burris TP. Suppression of TH17 differentiation and autoimmunity by a synthetic ROR ligand. *Nature*. 2011; 472:491–494. [PubMed: 21499262]
29. Marciano DP, Kuruvilla DS, Boregowda SV, Asteian A, Hughes TS, Garcia-Ordóñez R, Corzo CA, Khan TM, Novick SJ, Park H, Kojetin DJ, Phinney DG, Bruning JB, Kamenecka TM, Griffin PR. Pharmacological repression of PPAR $\gamma$  promotes osteogenesis. *Nature communications*. 2015; 6:7443.
30. Jin L, Martynowski D, Zheng S, Wada T, Xie W, Li Y. Structural basis for hydroxycholesterols as natural ligands of orphan nuclear receptor ROR $\gamma$ . *Mol Endocrinol*. 2010; 24:923–929. [PubMed: 20203100]
31. Goswami D, Callaway C, Pascal BD, Kumar R, Edwards DP, Griffin PR. Influence of domain interactions on conformational mobility of the progesterone receptor detected by hydrogen/deuterium exchange mass spectrometry. *Structure*. 2014; 22:961–973. [PubMed: 24909783]
32. West GM, Pascal BD, Ng LM, Soon FF, Melcher K, Xu HE, Chalmers MJ, Griffin PR. Protein conformation ensembles monitored by HDX reveal a structural rationale for abscisic acid signaling protein affinities and activities. *Structure*. 2013; 21:229–235. [PubMed: 23290725]
33. Pascal BD, Willis S, Lauer JL, Landgraf RR, West GM, Marciano D, Novick S, Goswami D, Chalmers MJ, Griffin PR. HDX workbench: software for the analysis of H/D exchange MS data. *J Am Soc Mass Spectrom*. 2012; 23:1512–1521. [PubMed: 22692830]

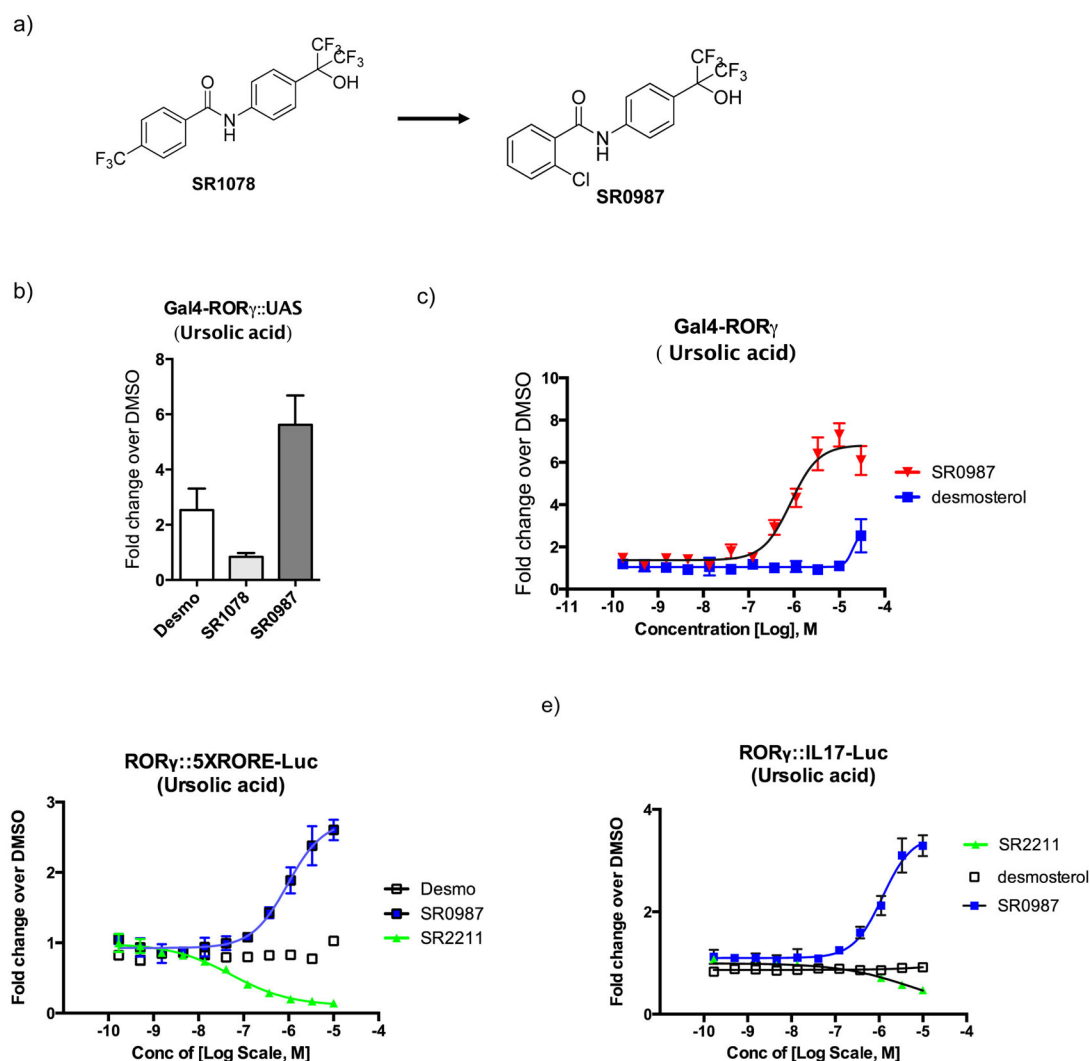
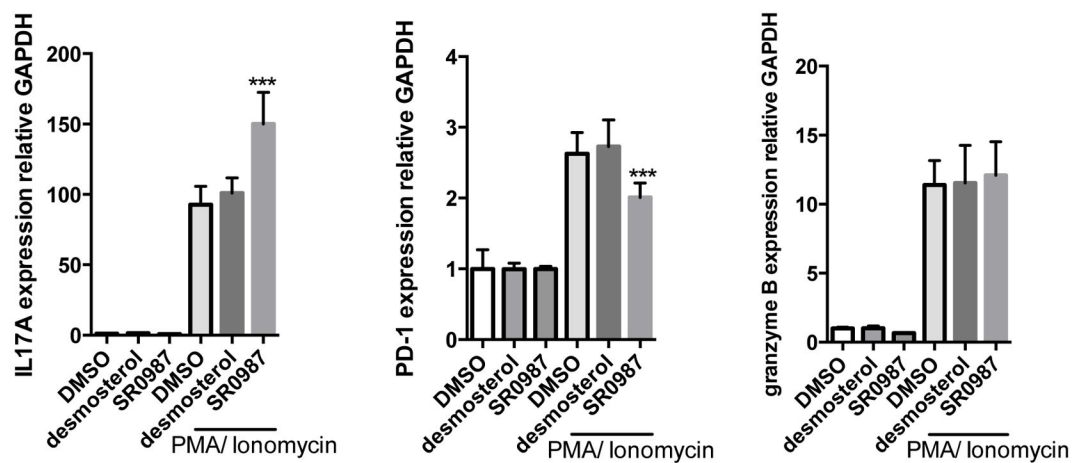


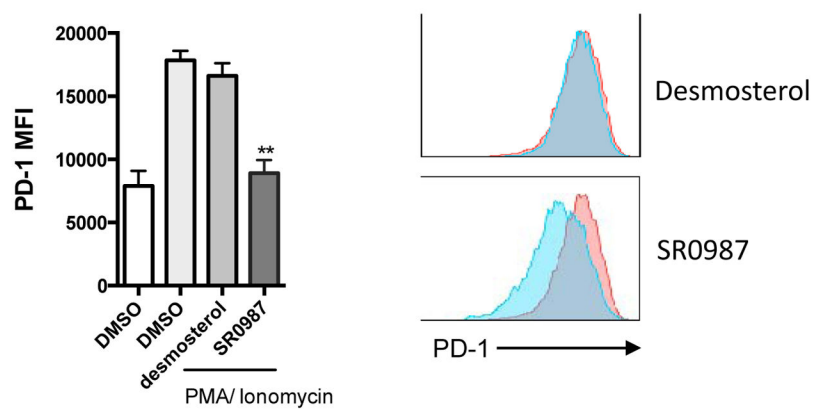
**Figure 1. In vitro characterization of synthetic ROR $\gamma$  agonist and endogenous ligand**

a) compound structure. b) ROR $\gamma$  agonist transactivation. Activation of Gal4-ROR $\gamma$ ::UAS-Luc reporter assay for SR1078, SR0987, and desmosterol at a 30  $\mu$ M concentration. c) concentration-response curve (CRC) for SR0987 and desmosterol in the presence of ursolic acid (2 $\mu$ M) in the Gal4-ROR $\gamma$ ::UAS-Luc reporter assay in HEK293T cells (right panel). All error bars denote s.e.m. d) Activation of full-length ROR $\gamma$  in the presence of ursolic acid (2 $\mu$ M) in HEK293T cells and co-transfected with 5XRORE-Luc reporter. e) Activation of full-length ROR $\gamma$  receptor in the presence of ursolic acid (2 $\mu$ M) in HEK293T cells and co-transfected with IL17-Luc reporter.

a)



b)



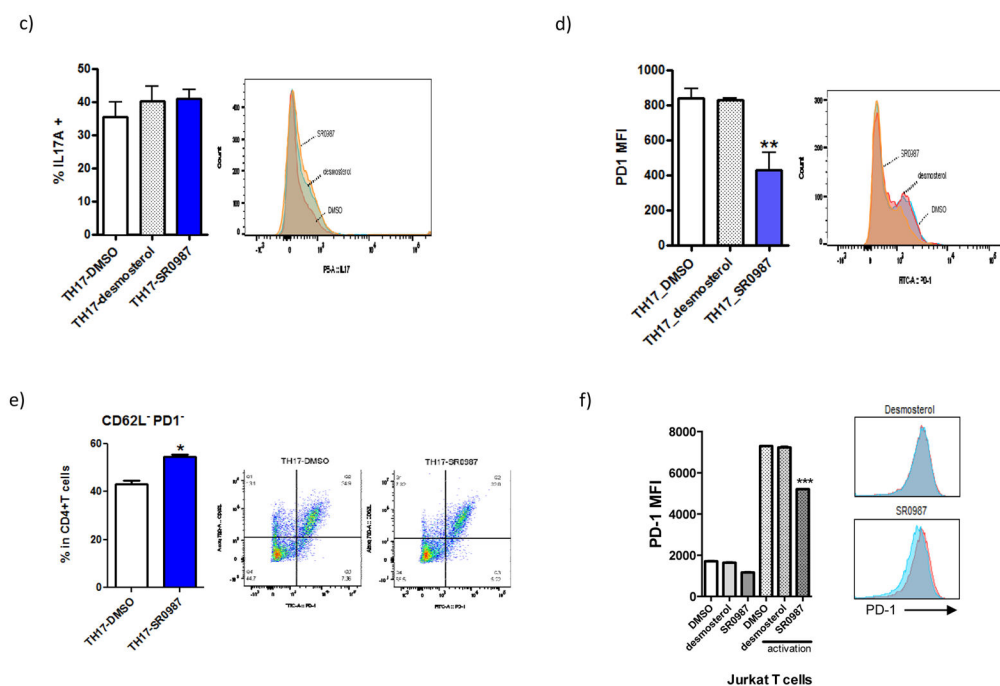


**Figure 2. Decreasing PD-1 by synthetic ROR $\gamma$ t agonist**

a) IL17A, PD-1 and granzyme B mRNA expression in stimulated EL4 cells (activated with PMA/Ionomycin treatment for 5 hr). b) PD-1 surface expression in EL4 cells. Cells were pretreated with compound (desmosterol, SR0987) for 48 hr. c) intracellular staining of IL17A in T<sub>H</sub>17 cells. d) cell surface expression of PD-1. e) CD62L-PD1- cell population. f) PD-1 expression in human Jurkat T cells.

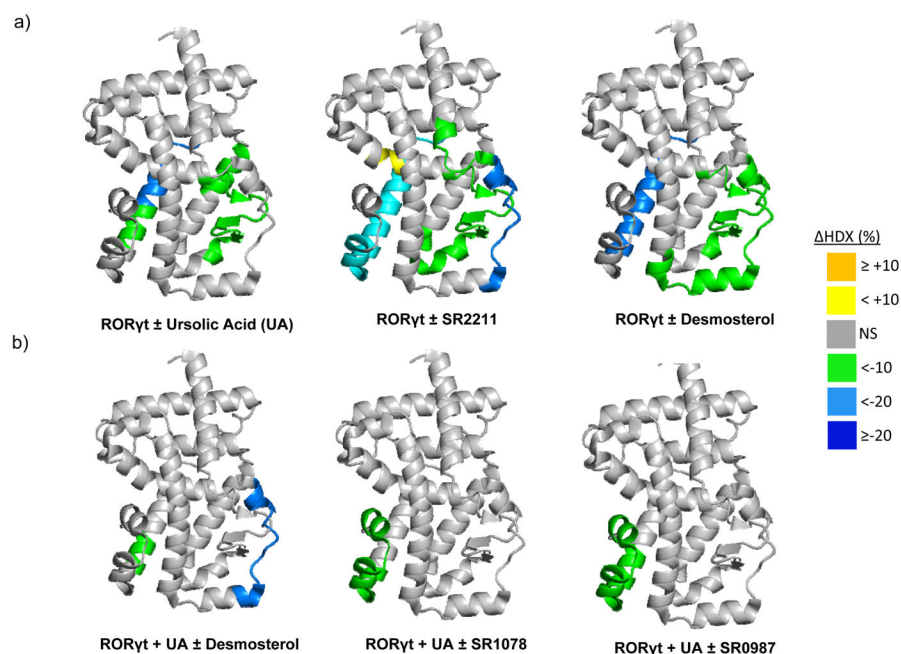


**Figure 3. Conformational Dynamics Probed by HDX**

a) Differential HDX kinetics of ROR $\gamma$ t LBD  $\pm$  compounds plotted over the crystal structure PDB:3LOL. b) Differential HDX kinetics of ursolic acid treated ROR $\gamma$ t LBD  $\pm$  compounds plotted over the crystal structure PDB:3LOL. Residues are colored corresponding to the average percent change in deuteration between apo and ligand bound ROR $\gamma$ t LBD over 6 time points (10, 30, 60, 300, 900, and 3600 seconds) run in triplicate ( $n = 3$ ) using the color scale bar shown. Cool colors are increased protection to solvent exchange (increased stabilization) and warm colors are decreased protection to solvent exchange (decreased stabilization). Grey color represents no statistically significant change (NS) observed in this region in HDX data sets comparing apo and ligand-bound receptor as determined using a paired two-tailed student's t-test ( $p < 0.05$ ).